

Research Article

Downregulation of hsa-miR-135b-5p Inhibits Cell Proliferation, Migration, and Invasion in Colon Adenocarcinoma

Yunxin Zhang , Wentao Zhang , Wenlong Xia , Junwei Xia , and Haishan Zhang 

Department of Gastrointestinal Colorectal and Anal Surgery, China-Japan Union Hospital of Jilin University, Changchun, Jilin 130033, China

Correspondence should be addressed to Haishan Zhang; yxinzhang@jlu.edu.cn

Received 7 July 2022; Accepted 8 October 2022; Published 21 October 2022

Academic Editor: Hongda Liu

Copyright © 2022 Yunxin Zhang et al. This is an open access article distributed under the Creative Commons Attribution License, which permits unrestricted use, distribution, and reproduction in any medium, provided the original work is properly cited.

Colon cancer is the most common malignant tumor of the gastrointestinal tract, and approximately 80%–90% of colon cancers are colon adenocarcinomas (COADs). This study aimed to screen key microRNAs (miRNAs) associated with COAD. Differentially expressed (DE) miRNAs were screened between COAD and adjacent cancer samples based on the Gene Expression Omnibus (GEO) and the Cancer Genome Atlas obtained from datasets. The miRNAs of interest were validated using quantitative real-time polymerase chain reaction. Moreover, the effects of hsa-miR-135b-5p on the biological behavior of COAD cells were observed. To obtain the target genes of hsa-miR-135b-5p, transcriptome sequencing of the SW480 cells was performed, followed by protein-protein interaction (PPI) network and hsa-miR-135b-5p-target gene regulatory network construction and prognostic analysis. Downregulation of hsa-miR-135b-5p significantly inhibited SW480 cell proliferation, migration, and invasion and significantly facilitated apoptosis ($P < 0.05$). A total of 3384 DEmRNAs were screened, and enrichment analysis showed that the upregulated mRNAs were enriched in 25 Kyoto Encyclopedia of Genes and Genomes (KEGG) pathways and 326 Gene Ontology Biological Processes (GO-BPs) while the downregulated mRNAs were enriched in 20 KEGG pathways and 276 GO-BPs. A PPI network was then constructed, and H2BC14, H2BC3, and H4C11 had a higher degree. In addition, a total of 352 hsa-miR-135b-5p-gene regulatory relationships were identified. Prognostic analysis showed that *FOXN2*, *NSA2*, *MYCBP*, *DIRAS2*, *DES11*, and *RAB33B* had prognostic significance ($P < 0.05$). In addition, the validation analysis results showed that *FOXN2*, *NSA2*, and *DES11* were significantly expressed between the miR-135b-5p-inhibitor and negative control groups ($P < 0.05$). Therefore, downregulation of hsa-miR-135b-5p inhibits cell proliferation, migration, and invasion in COAD, and carcinogenesis may function by targeting *FOXN2*, *NSA2*, *MYCBP*, *DIRAS2*, *DES11*, and *RAB33B*.

1. Introduction

Colon cancer is the most common malignant tumor in the gastrointestinal tract and ranks third and second in terms of morbidity and mortality, respectively, among all solid cancers [1–3]. Approximately 80–90% of colon cancers are colon adenocarcinomas (COADs) based on pathologic classification [4, 5]. In China, due to the increase in poor living and dietary habits, the incidence rate of COAD has also been increasing [6]. More than 83% of patients with COAD are at an advanced stage upon diagnosis, and nearly half of them are accompanied by metastasis from other sites and have a poor prognosis [7]. Surgical treatment is the most effective treatment for COAD; however, the effect of surgical

resection is closely related to the preoperative staging of patients [8, 9]. Thus, further studies on the molecular mechanism of COAD occurrence and development and exploration of new key molecules may provide novel ideas for the treatment of COAD.

MicroRNAs (miRNAs) are non-coding RNAs 20–24 nt long and regulate target gene expression by binding to the 3' untranslated region of the target gene, which affects a series of physiological processes [10]. Studies have revealed that miRNAs are involved in almost all signaling pathway regulations in cancer and that there are differences in tumor diagnosis, staging, progression, prognosis, and chemotherapy [11–13]. Uncontrolled proliferation is a major feature of cancer and is the basis of its development [14]. As regulators,

miRNAs affect tumor growth by targeting key members of the COAD-related proliferation signaling pathway [15]. The expression of many miRNAs is different between normal and COAD tissues. For instance, Mi et al. revealed that high miR-31-5p expression facilitated COAD progression by targeting TNS1 [16]. Zhao and Qin found that miRNA-708, which targets *ZNF549*, regulates COAD development through the PI3K/Akt pathway [17]. Liu and Di Wang revealed that miR-150-5p inhibits *TP53* to facilitate the proliferation of COAD [18]. Therefore, screening for novel miRNAs in COAD is important.

Therefore, this study was conducted to explore the key miRNAs correlated with the development of COAD as well as the molecular mechanisms involved. First, the common differentially expressed (DE) miRNAs were screened between COAD and adjacent cancer samples based on the Gene Expression Omnibus (GEO) and the Cancer Genome Atlas (TCGA) datasets. In addition, miRNAs of interest were verified using quantitative reverse transcription polymerase chain reaction (qRT-PCR), and hsa-miR-135b-5p was screened. Moreover, the effects of hsa-miR-135b-5p on the biological behavior of COAD cells were observed, and transcriptome sequencing was performed to identify target genes of hsa-miR-135b-5p. This study provides new clues for the treatment of COAD. A flowchart of the study is presented in Figure 1.

2. Materials and Methods

2.1. Data Acquisition and Preprocessing. The processed miRNA expression profile data of the GSE125961 dataset (six COAD tissues and six adjacent cancer tissues) were downloaded from the GEO database (<https://www.ncbi.nlm.nih.gov/geo/>), after which the miRNA data were normalized. TCGA-COAD miRNA data (450 COAD samples and eight adjacent cancer samples) were also obtained from the University of California, Santa Cruz, database (<https://xenabrowser.net/datapages/>), and the miRNAID was converted to the mature miRNA ID of the V21 version.

2.2. Identification of DE miRNAs. After data preprocessing, DE miRNAs were identified between COAD and adjacent cancer samples using the “limma” package (version 3.10.3) [19], with the threshold set at $P < 0.05$ and $|\log \text{fold change (FC)}| > 2$. Moreover, overlapping DE miRNAs screened from the GEO and TCGA datasets were obtained.

2.3. miRNA-Target Gene Regulatory Network Construction. miRWalk3.0 [20] was used to predict the target genes of the overlapping DE miRNAs in the miRTarBase, TargetScan, and miRDB databases. The target genes in all three databases were then obtained to build a miRNA-target gene regulatory network using Cytoscape (version 3.2.0) [21].

2.4. Sample Collection. The 20 COAD and corresponding paracancerous tissues (including seven females and 13 males aged 46–78 years) were obtained from the China-Japan

Union Hospital of Jilin University. This study was approved by the ethics committee of the China-Japan Union Hospital of Jilin University (N:2021081011). Informed consent was obtained from all subjects.

2.5. Cell Culture and Transfection. Human COAD cell lines (SW480, HT29, and HCT116) and a human colon epithelial cell line (NCM460) were purchased from Procell Life Science & Technology Co. NCM460 cells were cultured in 90% Dulbecco's Modified Eagle Medium: F12; SW480 cells were cultured in 90% L-15 base medium; and HT29 and HCT116 cells were cultured in 90% McCoy's 5A base medium. The cells were supplemented with 10% fetal bovine serum and 1% penicillin-streptomycin solution at 37°C in 95% air and 5% CO₂, which was then replaced with a complete medium, and the cells were cultured for 24–48 h. The cells were then transfected with hsa-miR-135b-5p inhibitors or a negative control using Lipofectamine 2000 following the manufacturer's instructions (incubation at room temperature for 20 min).

2.6. qRT-PCR. Total RNA was extracted using TRIzol, and RNA concentration and quality were determined using a microplate reader (Infinite M100 PRO; TECAN, Switzerland). Total RNA was reverse-transcribed using a reverse transcription kit (MR101-01; Vazyme Biotech Co., Ltd., China), and the cDNA was used for qRT-PCR. snRNA U6 was used as an internal reference. The primer sequences are listed in Table 1.

2.7. Cell Counting Kit-8 (CCK8) Assay. After 0, 24, 48, or 72 h of incubation, cell viability was analyzed using CCK8 (C0037; Beyotime, China). The cells were first cultured in an incubator at 37°C and with 5% CO₂ for 0, 24, 48, or 72 h, followed by treatment with CCK8 (20 μL per well) at 37°C for 2 h. OD450 was measured using a microplate reader (Infinite M100 PRO; TECAN). Each experiment was performed in triplicate.

2.8. Flow Cytometry. After transfection with hsa-miR-135b-5p inhibitors or the negative control, the cells were collected in a flow tube, washed with phosphate-buffered saline (PBS), and then centrifuged. Cell apoptosis was assessed using an Annexin V/fluorescein isothiocyanate (FITC) and propidium iodide (PI) apoptosis detection kit (C1062L; Beyotime) according to the manufacturer's instructions. Annexin V-FITC, PI, and 4-(2-hydroxyethyl)-1-piperazineethanesulfonic acid buffer were mixed at a ratio of 1 : 2 : 5 to make a dye liquor, of which 100 μL was used to resuspend 1×10^6 cells. Cell apoptosis was analyzed using FlowJo software. Each experiment was performed in triplicate.

2.9. Transwell Assay. After transfection with hsa-miR-135b-5p inhibitors or the negative control, the cells were collected and centrifuged. A transwell assay was

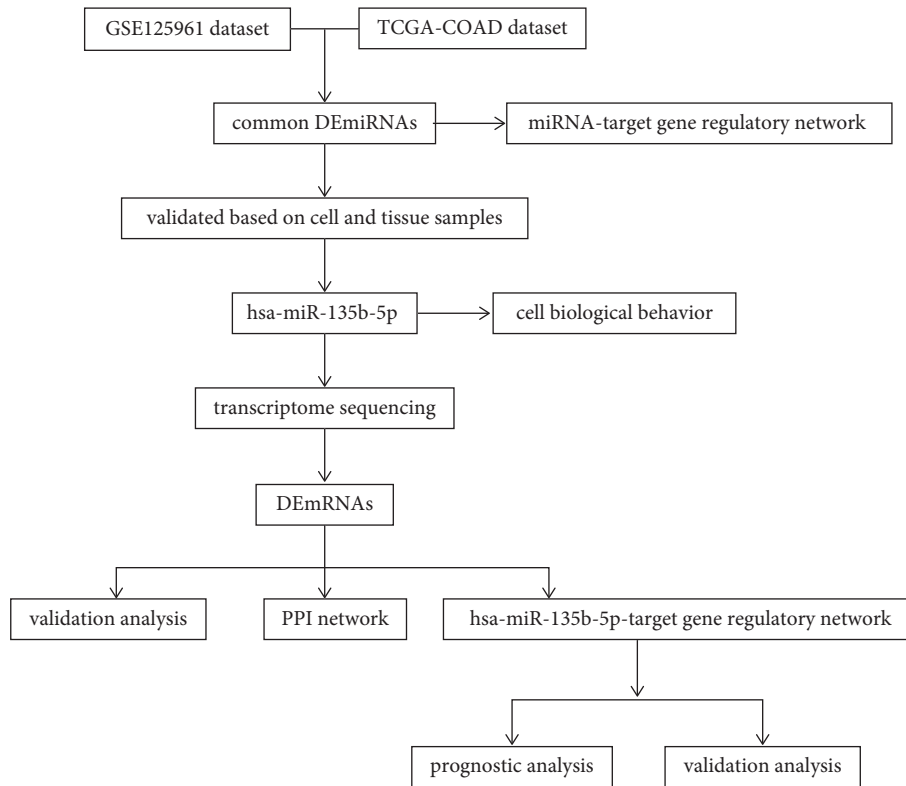


FIGURE 1: Flowchart of this study.

TABLE 1: The sequences of primers.

Name	Sequences (5'-3')
hsa-miR-135b-5p(RT)	GTCGTATCCAGTGCAGGGTCCGAGGTATTCGCACTGGATACGACTCACAT
hsa-miR-135b-5p(F)	CGCGTATGGCTTTTCATTCT
hsa-miR-135b-5p(R)	AGTGCAGGGTCCGAGGTATT
hsa-miR-19a-3p(RT)	GTCGTATCCAGTGCAGGGTCCGAGGTATTCGCACTGGATACGACTCAGTT
hsa-miR-19a-3p(F)	GCGTGTGCAAATCTATGCAA
hsa-miR-19a-3p(R)	AGTGCAGGGTCCGAGGTATT
hsa-miR-33a-5p(RT)	GTCGTATCCAGTGCAGGGTCCGAGGTATTCGCACTGGATACGACTGCAAT
hsa-miR-33a-5p(F)	CGCGTGCATGTAGTTGC
hsa-miR-33a-5p(R)	AGTGCAGGGTCCGAGGTATT
hsa-miR-328-3p(RT)	GTCGTATCCAGTGCAGGGTCCGAGGTATTCGCACTGGATACGACACGGAA
hsa-miR-328-3p(F)	GCTGGCCCTCTCTGCCC
hsa-miR-328-3p(R)	AGTGCAGGGTCCGAGGTATT
hsa-miR-139-5p(RT)	GTCGTATCCAGTGCAGGGTCCGAGGTATTCGCACTGGATACGACTGGA
hsa-miR-139-5p(F)	CGCGTCTACAGTGCACGTGTC
hsa-miR-139-5p(R)	AGTGCAGGGTCCGAGGTATT
hsa-miR-490-3p(RT)	GTCGTATCCAGTGCAGGGTCCGAGGTATTCGCACTGGATACGACCAGCAT
hsa-miR-490-3p(F)	CGCAACCTGGAGGACTCC
hsa-miR-490-3p(R)	AGTGCAGGGTCCGAGGTATT
snRNA U6(R)	AACGCTTACGAATTTGCGT
snRNA U6(F)	CTCGCTTCGGCAGCACACA
FOXN2(R)	GCTGACTCACTGTCCACTAGAG
FOXN2(F)	AGAGAGCTGAAACCCAGGAG
RAB33B(R)	GTCTCGGAAATCCACCCCTA
RAB33B(F)	TGATCGGCGACTCCAATGTG
NSA2(R)	GCTTAGCCTTCAGACCAATCATT
NSA2(F)	CACCGTAAACGCTATGGATACC
DIRAS2(R)	CTCTCCACGTCCCCTTTGA
DIRAS2(F)	TTACCAGCCGACAGTCCTTG
DES11(R)	GCCGAAGAAGAACTCATCCTTGT
DES11(F)	CCGAATCTCTATCCGGTGAAGC

performed to detect cell migration and invasion, as described previously [22]. After incubation at 37°C for 16 h, the transwell chamber was washed with PBS and fixed in 95% ethanol for 5 min. The cells were stained with crystal violet for 10 min, washed with PBS, and analyzed under an optical microscope (IX73; Olympus, Japan) using ImageJ software. Each experiment was performed in triplicate.

2.10. Transcriptome Sequencing. Total RNA was obtained from hsa-miR-135b-5p inhibitor or negative control-transfected SW480 cells using TRIzol reagent. RNA integrity, purity, and concentration were determined using NanoDrop2000. Sequencing libraries were generated using NEBNext® Ultra™ RNA Library Prep Kit for Illumina® (E7530S; New England Biolabs, USA) according to the manufacturer's instructions, and index codes were added to attribute sequences to each sample. Sequencing was performed on an Illumina sequencing platform with the PE300 bp sequencing mode. After cluster generation, the library preparations were sequenced on an Illumina HiSeq platform, and paired-end reads were generated. Quality control of the reads was conducted using in-house written scripts. Raw reads in FASTQ format were processed using in-house Perl scripts. Transcriptome sequencing data were uploaded to the National Center for Biotechnology Information database using the BioProject ID PRJNA870261.

2.11. Identification of DEmRNAs. Raw counts were normalized using the median ratio method in the “DESeq2” package (version 1.18.1) [23], and differential expression analysis was performed to identify DEmRNAs between the hsa-miR-135b-5p inhibitor and negative control groups using the Wald test with cutoff values of $P < 0.05$ and $|\log_2 FC| \geq 1$. In addition, enrichment analysis was performed on the identified up and downregulated mRNAs using the “clusterProfiler” package (version 3.2.11) [24] in R (version 3.4.4) with a threshold of $P_{\text{adjust}} < 0.05$, and $\text{count} \geq 2$. The Benjamini and Hochberg method was used to adjust the P value.

2.12. Protein-Protein Interaction (PPI) Network. A PPI network of the top 50 upregulated and downregulated mRNAs was built using the STRING database (version 11) [25], and the parameters were set as follows: species, Homo sapiens; and PPI score > 0.4 .

2.13. hsa-miR-135b-5p-Target Gene Regulatory Network Construction. miRWalk3.0 [20] was used to identify the target genes of hsa-miR-135b-5p in miRWalk, miRtarbase, TargetScan, and miRDB databases. Target genes with a score ≥ 0.9 in more than two databases were acquired and intersected with the DEmRNAs, after which overlapping mRNAs were obtained. A regulatory network was then constructed using Cytoscape (version 3.6.1) [21].

2.14. Prognostic Analysis. The gene expression of RNA sequencing ($\log_2(\text{fpkm} + 1)$) and clinical data (TCGA Colon and Rectal Adenocarcinoma (COADREAD) Phenotype) of Genomic Data Commons (GDC) TCGA (cohort: GDC Pan-Cancer) were obtained from the TCGA database [26]. Then, the matrix data of TCGA COADREAD mRNA and the clinical information of overall survival time in miRNA-target were acquired. The “survival” package (version 2.42–6) [27] in R (version 3.4.4) was used to perform prognostic analysis with a threshold of $P < 0.05$.

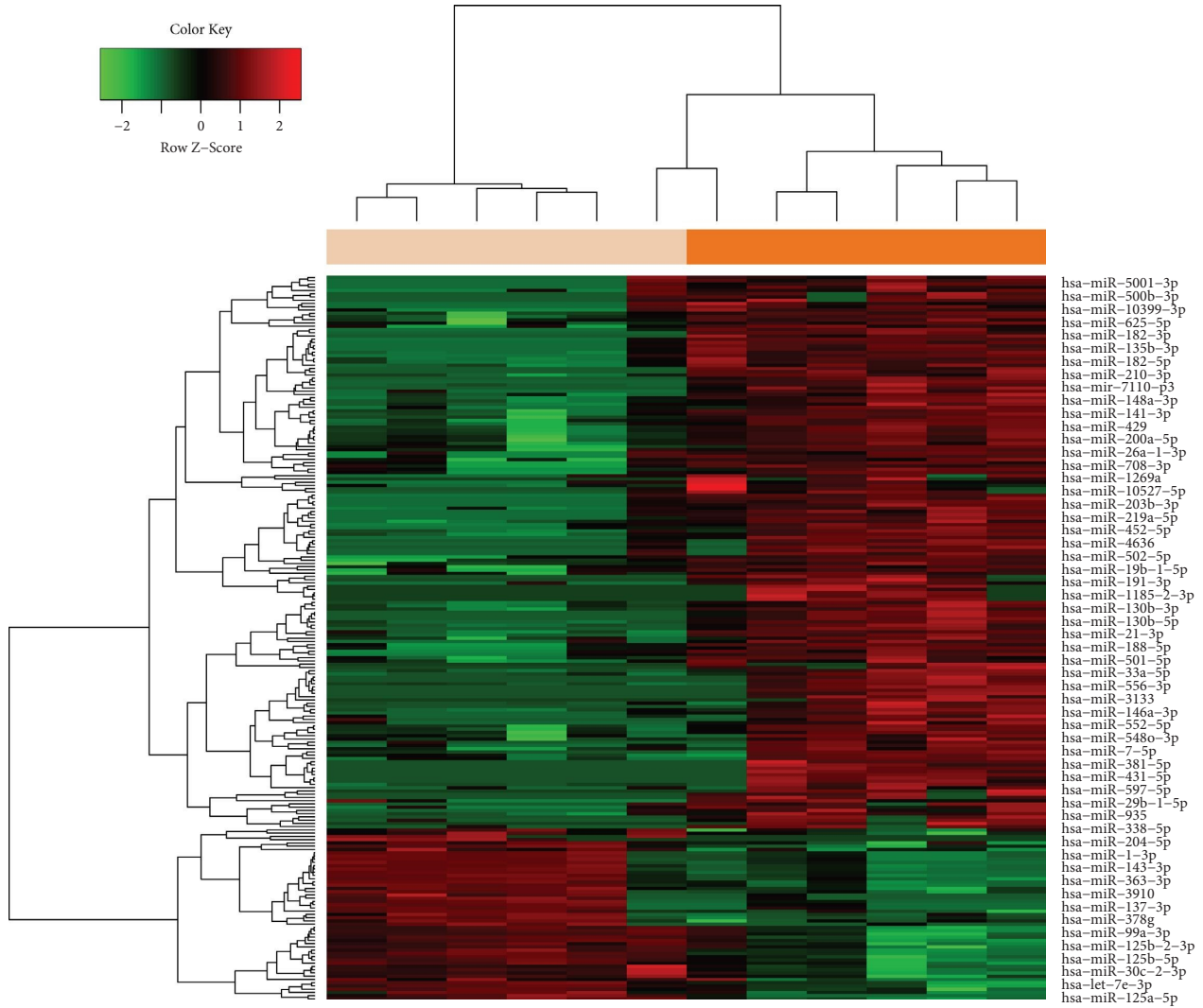
2.15. Statistical Analysis. SPSS 22.0 software was used for statistical analysis. One-way analysis of variance and Newman–Keuls multiple comparison tests were used to compare the differences between groups. Statistical significance was set at $P < 0.05$.

3. Results and Discussion

3.1. DEmiRNAs and miRNA-Target Gene Regulatory Network. According to the cutoff value of $P < 0.05$ and $|\log FC| > 2$, 223 DEmiRNAs (170 upregulated and 53 downregulated) and 134 DEmiRNAs (60 upregulated and 74 downregulated) were identified from the GEO and TCGA datasets, respectively (Figures 2(a) and 2(b)). A total of 26 overlapping DEmiRNAs were obtained, including 17 upregulated and nine downregulated miRNAs (Figure 2(c)). In addition, a total of 194 miRNA-target gene regulatory relationships were acquired, including 17 miRNAs and 188 genes (Figure 3).

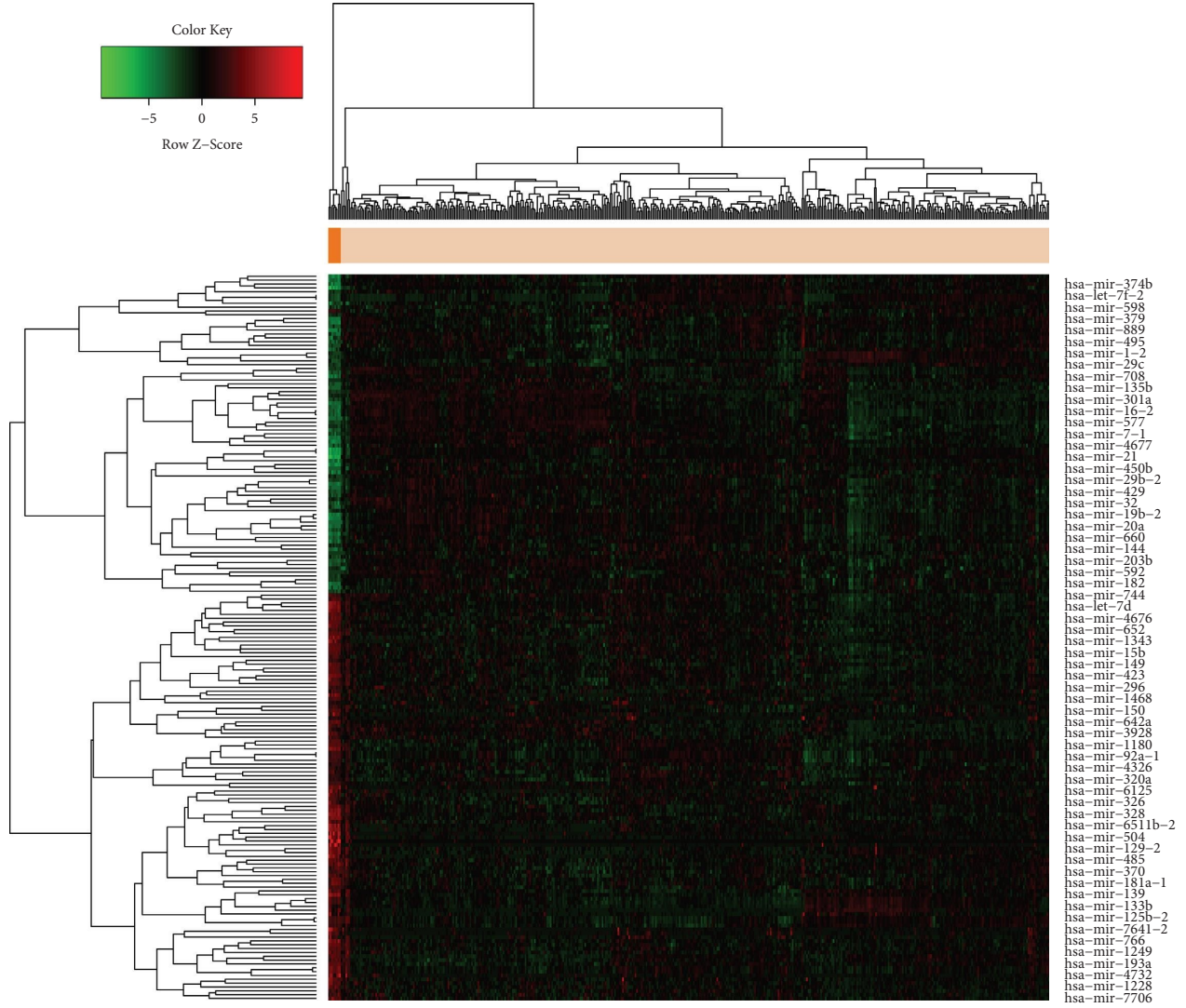
3.2. High hsa-miR-135b-5p Expression in COAD. Of the 26 overlapping DEmiRNAs, six miRNAs that were not reported in COAD were selected, namely, hsa-miR-135b-5p, hsa-miR-19a-3p, hsa-miR-33a-5p, hsa-miR-328-3p, hsa-miR-139-5p, and hsa-miR-490-3p. qRT-PCR was performed on tissue and SW480 cells, and the results showed that only hsa-miR-135b-5p expression was significantly higher in the tumor groups (both in cell and tissue samples) than in the control groups ($P < 0.05$; Figure 4(a)).

3.3. Experimental Observation of the Effect of hsa-miR-135b-5p. Experiments were performed to determine whether hsa-miR-135b-5p influences the biological behavior of COAD cells. The expression of hsa-miR-135b-5p was significantly reduced in the hsa-miR-135b-5p inhibitor group compared with the inhibitor negative control and control groups ($P < 0.05$; Figure 4(b)). In addition, the CCK8 assay results showed that after reducing hsa-miR-135b-5p expression, cell growth was significantly reduced ($P < 0.05$; Figure 4(c)). Transwell assays showed that migration and invasion of COAD cells were significantly inhibited after reducing hsa-miR-135b-5p expression ($P < 0.05$; Figure 4(d)). Meanwhile, flow cytometric analysis revealed that cell apoptosis was markedly increased after reducing hsa-miR-135b-5p expression ($P < 0.05$; Figure 4(e)).



(a)

FIGURE 2: Continued.



(b)
FIGURE 2: Continued.

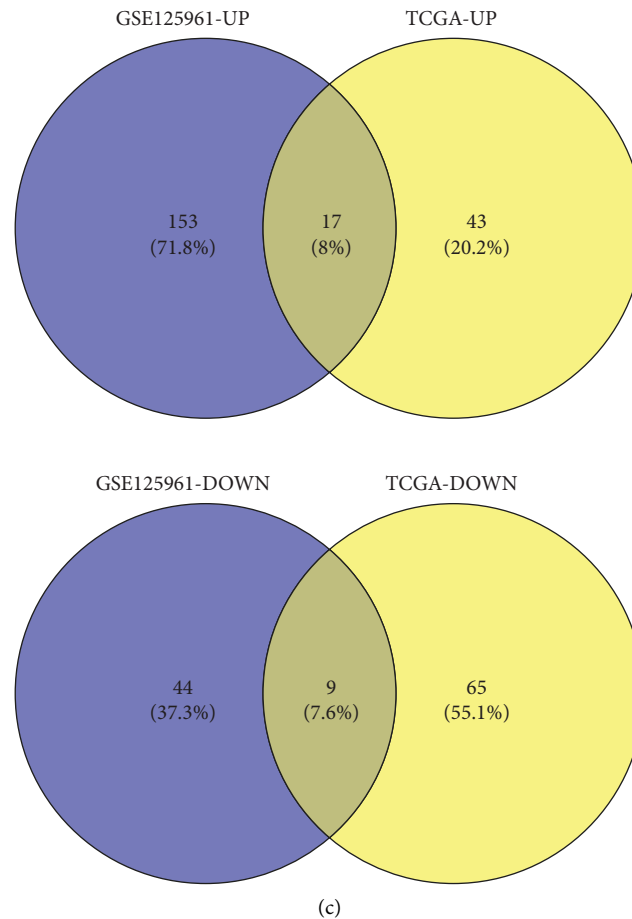


FIGURE 2: DEmiRNA screening and miRNA-target gene regulatory network. Heatmap of DEmiRNAs in the GEO (a) and TCGA datasets (b). The orange bar represents the normal group, and the yellow bar represents the tumor group. (c) The overlapped up and downregulated miRNAs screened from the GEO and TCGA datasets. DEmiRNA, differentially expressed microRNA; GEO, Gene Expression Omnibus; TCGA, the Cancer Genome Atlas.

3.4. Identification of DEmRNAs. A total of 3384 DEmRNAs (2012 upregulated and 1372 downregulated) were identified between the hsa-miR-135b-5p inhibitor and negative control groups (Figure 5(a)). Enrichment analysis showed that the upregulated mRNAs were enriched in 25 Kyoto Encyclopedia of Genes and Genomes (KEGG) pathways (e.g., ribosome, oxidative phosphorylation, and systemic lupus erythematosus) and 326 Gene Ontology Biological Processes (GO-BPs; e.g., signal recognition particle-dependent cotranslational protein targeting to membrane, cotranslational protein targeting to membrane, and protein targeting to endoplasmic reticulum) as shown in Figures 5(b) and 5(c), while the downregulated mRNAs were enriched in 20 KEGG pathways (e.g., extracellular matrix (ECM)-receptor interaction, protein digestion and absorption, and hematopoietic cell lineage) and 276 GO-BPs (e.g., cell-substrate adhesion, extracellular matrix organization, and extracellular structure organization) as shown in Figures 5(d) and 5(e).

3.5. PPI Network. A PPI network containing 45 nodes and 65 interaction pairs (Figure 6(a)) was constructed based on the identified DEmRNAs. H2BC14 (degree = 9), H2BC3

(degree = 9), and H4C11 (degree = 9) had higher degrees in the PPI network (Table 2).

3.6. hsa-miR-135b-5p-Target Gene Regulatory Network Construction. A total of 352 regulatory relationships were identified, and 10 overlapping genes were obtained (Figure 6(b)), namely, *NSA2*, *FOXN2*, *DIRAS2*, *DES11*, *SV2C*, *RAB33B*, *MCTS1*, *CNIH4*, *SLCO5A1*, and *MYCBP* (Figure 6(c)).

3.7. Prognostic Analysis. Prognostic analysis was conducted on the 10 overlapping genes, and the results showed that *FOXN2* ($P=0.0085$), *NSA2* ($P=0.044$), *MYCBP* ($P=0.0047$), *DIRAS2* ($P=0.0015$), *DES11* ($P=0.022$), and *RAB33B* ($P=0.037$) had prognostic significance ($P < 0.05$; Figure 7). Of them, *DIRAS2* was related to poor prognosis, while the other genes were related to better prognosis. Moreover, the six prognosis-related genes were validated, and the results showed that *FOXN2* expression was significantly reduced while *NSA2* and *DES11* expression was significantly increased in the miR-135b-5p-inhibitor group than in the negative control

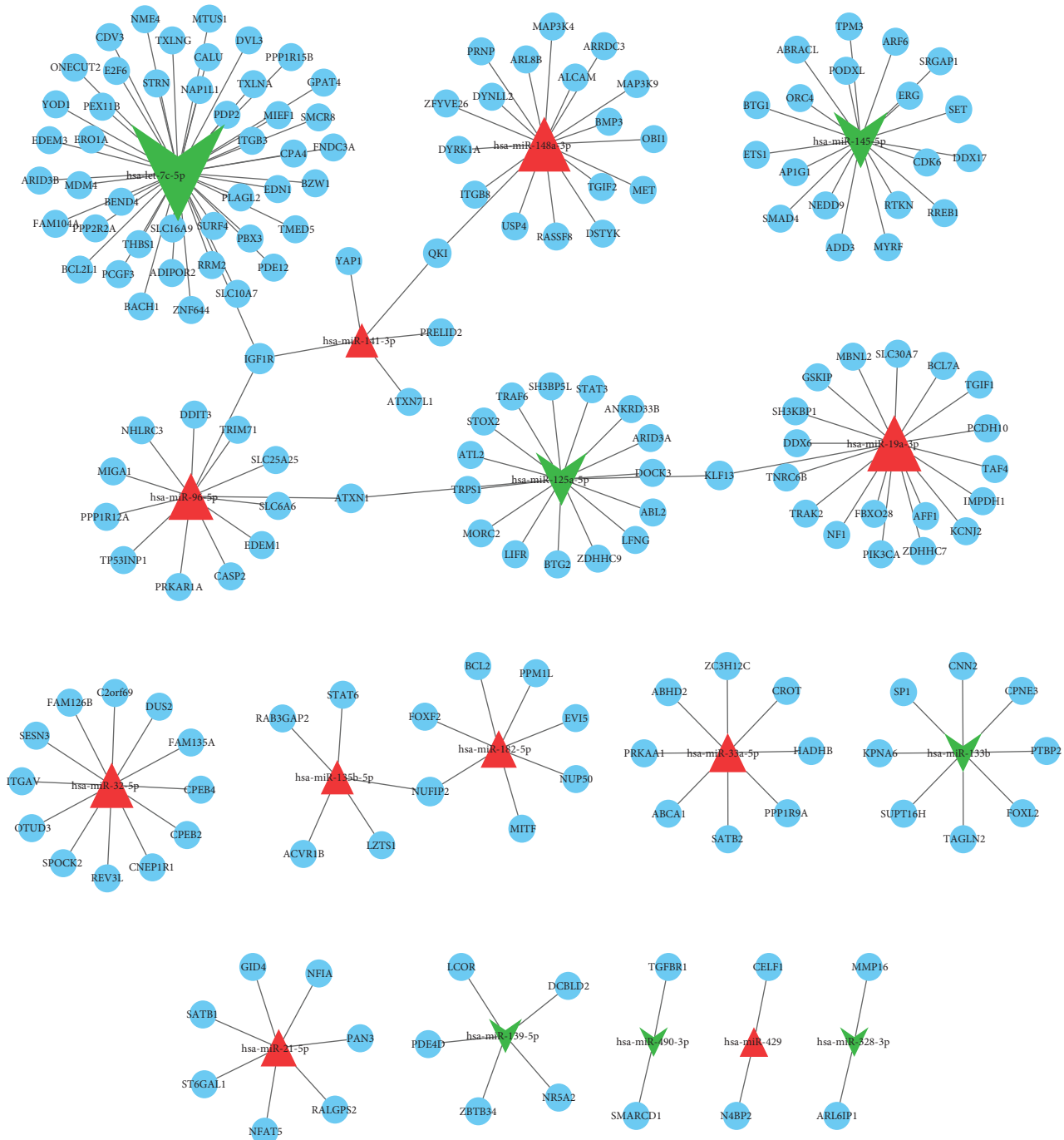


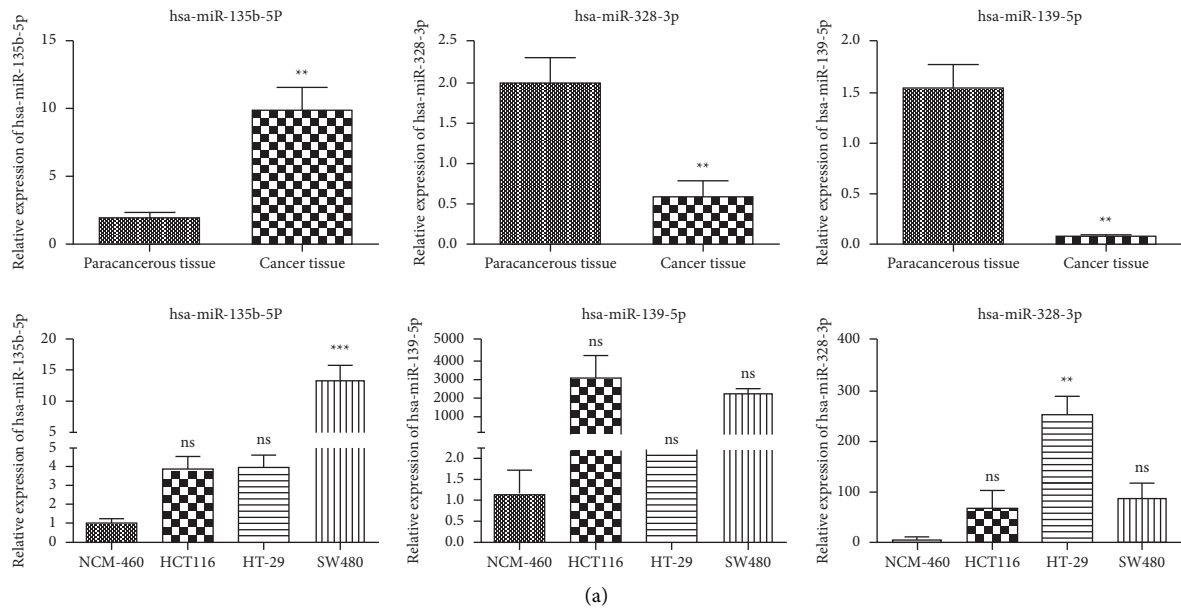
FIGURE 3: MiRNA-target gene regulatory network. The red triangle represents the upregulated miRNAs, the green arrow represents the downregulated miRNAs, and the blue circle represents the target genes. A bigger node size indicates a higher degree.

group (Figure 8). In contrast, *MYCBP* was not expressed in either group ($P < 0.05$).

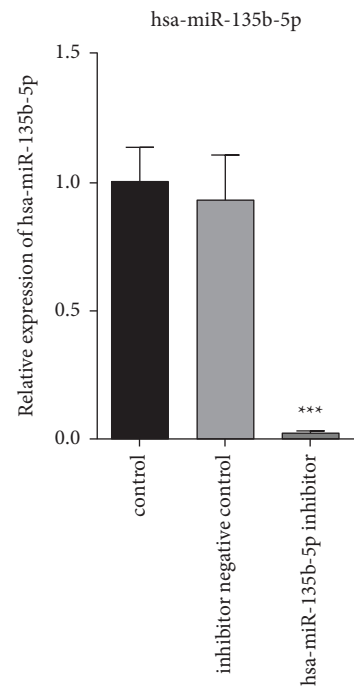
4. Discussion

Dysregulated miRNAs play crucial roles in tumorigenesis of human cancers [28, 29]. In this study, we found that downregulation of *hsa-miR-135b-5p* significantly inhibited SW480 cell proliferation, migration, and invasion and significantly facilitated apoptosis. In addition, a total of 3384

DEmRNAs were identified, and enrichment analysis showed that the upregulated mRNAs were enriched in 25 KEGG pathways and 326 GO-BPs and the downregulated mRNAs were enriched in 20 KEGG pathways and 276 GO-BPs. A PPI network was then constructed wherein H2BC14, H2BC3, and H4C11 had a higher degree. Furthermore, a total of 352 *hsa-miR-135b-5p*-gene regulatory relationships were identified. Prognostic analysis showed that *FOXN2*, *NSA2*, *MYCBP*, *DIRAS2*, *DESII*, and *RAB33B* have prognostic significance.

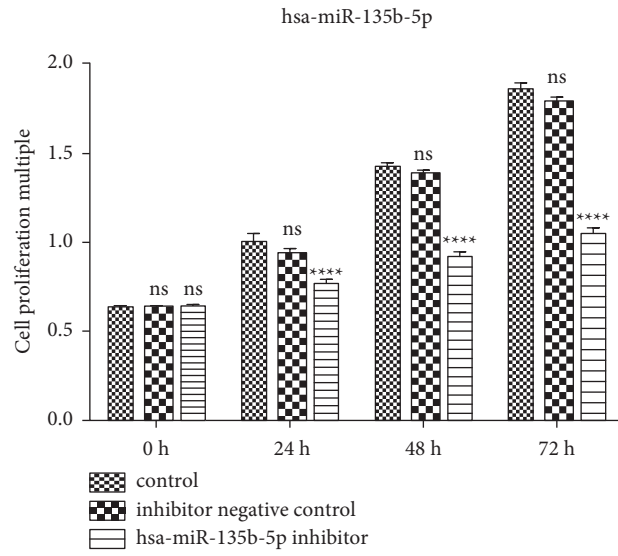


(a)

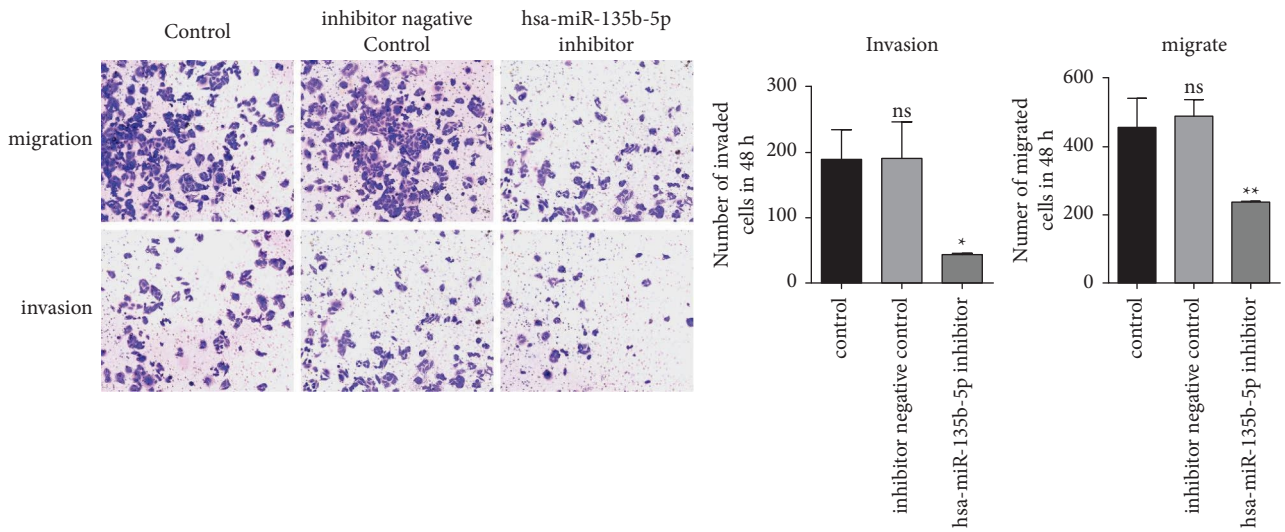


(b)

FIGURE 4: Continued.

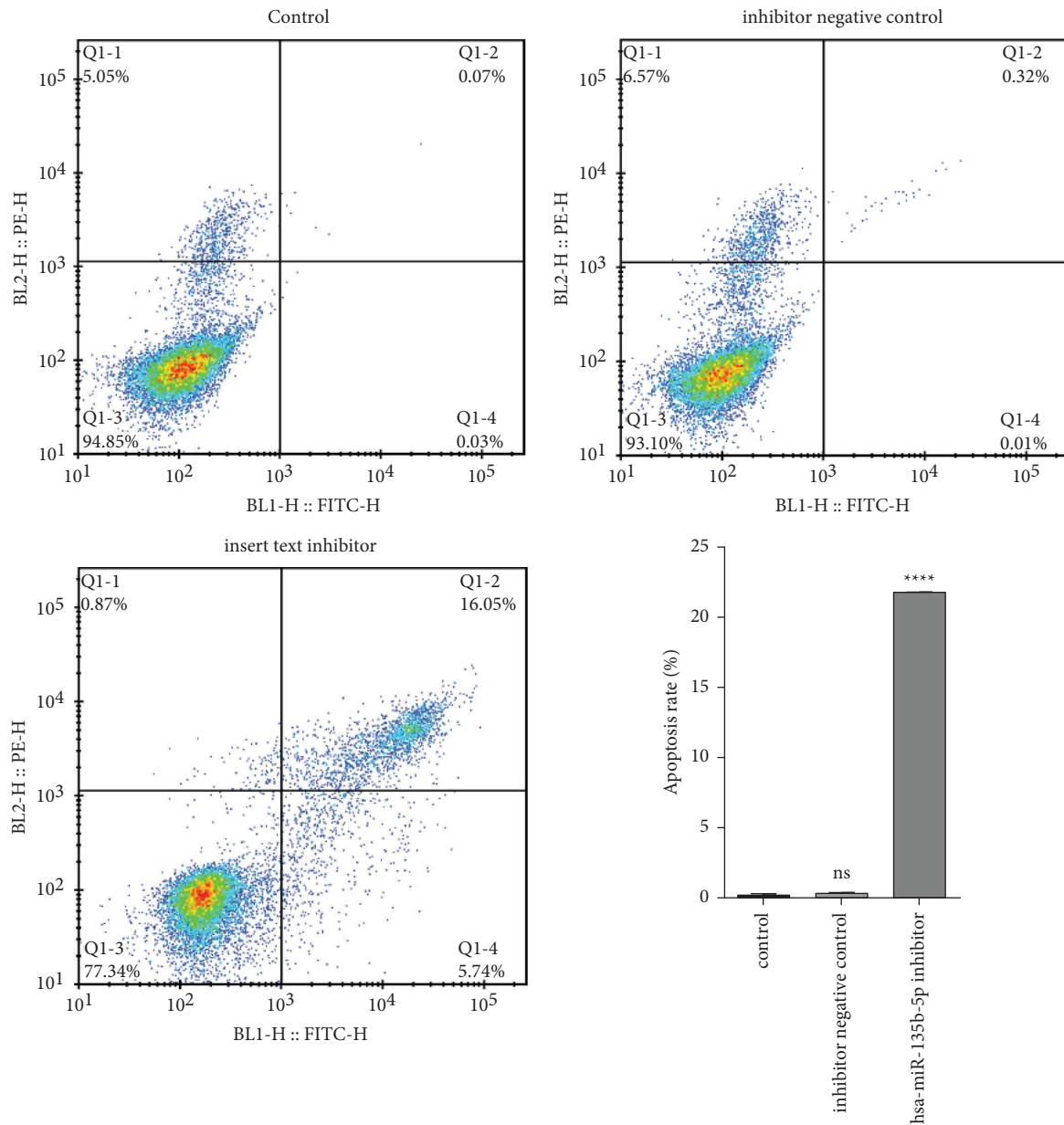


(c)



(d)

FIGURE 4: Continued.



(e)

FIGURE 4: Effect of hsa-miR-135b-5p knockdown on COAD. (a) Relative expression levels of hsa-miR-135b-5p in COAD tissue and cell samples. (b) Transfection efficiency. (c) Effect of reduced hsa-miR-135b-5p levels on SW480 cell proliferation. (d) Effect of reduced hsa-miR-135b-5p levels on SW480 cell migration and invasion. (e) Effect of reduced hsa-miR-135b-5p levels on SW480 cell apoptosis. * $P < 0.05$, ** $P < 0.01$, *** $P < 0.001$, **** $P < 0.0001$, and “ns” represents no significant difference.

We first used miRNA expression profile data to screen the DE miRNAs in COAD and adjacent cancer samples, and a total of 26 overlapping DE miRNAs were obtained from the GEO and TCGA datasets. Six miRNAs of interest were selected among the 26 overlapping DE miRNAs for validation via qRT-PCR, and the results showed that only hsa-miR-135b-5p was expressed at significantly higher levels in the tumor groups than in the control groups. Numerous studies have reported that hsa-miR-135b-5p is dysregulated in many human cancers and plays a crucial role in cancer progression. Naorem et al. demonstrated that hsa-miR-135b-5p is dysregulated in triple-negative breast cancer [30].

Lazzarini et al. showed that hsa-miR-135b-5p is differentially expressed in normal myometrium and leiomyomas [31]. Magalhães et al. found that in both diffuse and intestinal gastric cancer subtypes, APC is modulated by hsa-miR-135b-5p [32]. However, hsa-miR-135b-5p in COAD has not yet been reported. In this study, our *in vitro* experiments revealed that changes in hsa-miR-135b-5p expression influenced the biological behavior of COAD cells. Down-regulation of hsa-miR-135b-5p resulted in significantly reduced growth, migration, and invasion and markedly increased apoptosis of COAD cells, which may provide novel insights into the treatment of COAD.

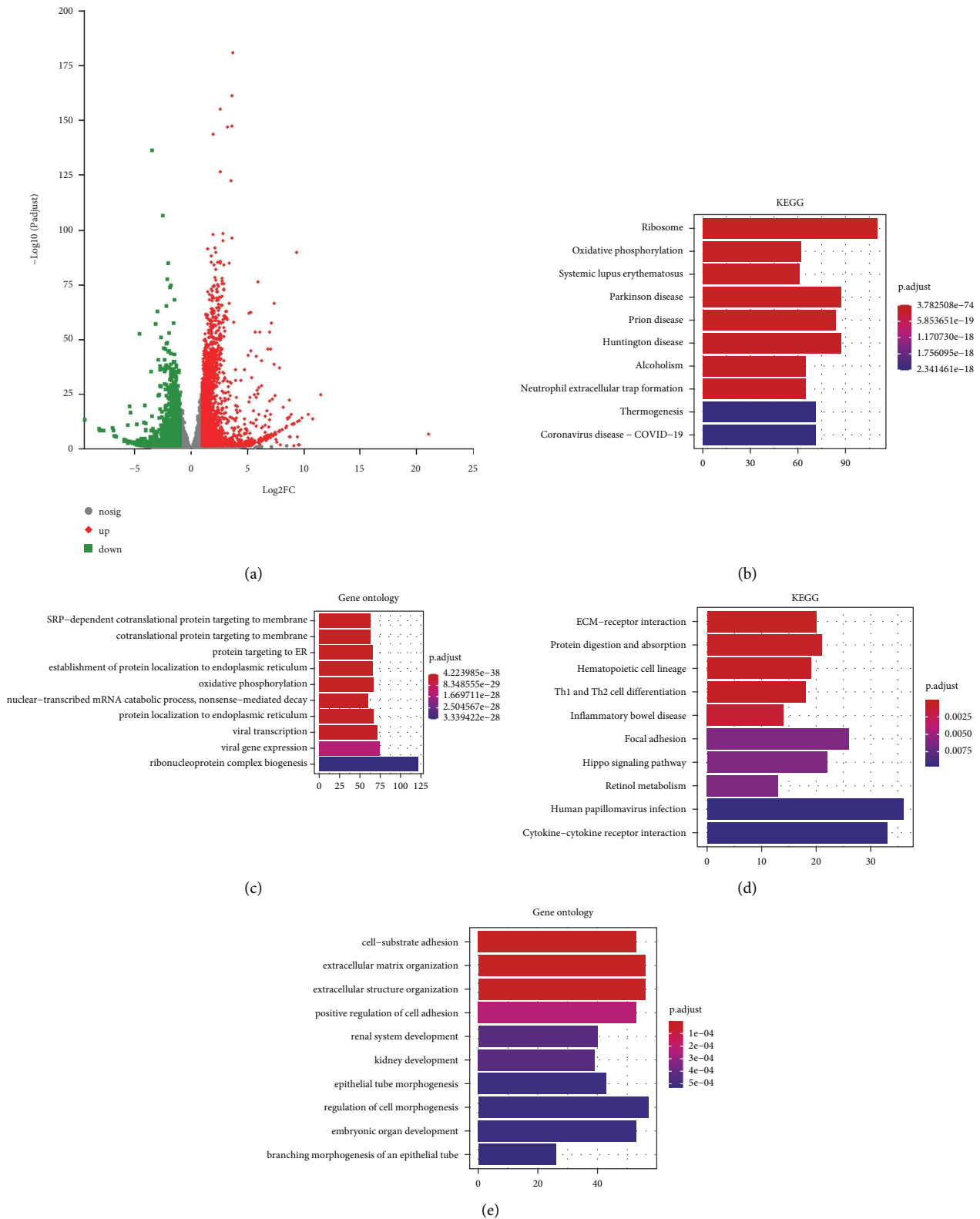


FIGURE 5: DE mRNAs between the hsa-miR-135b-5p inhibitor and negative control groups. (a) DE mRNAs between the hsa-miR-135b-5p inhibitor and negative control groups. Top 10 significantly enriched KEGG (b) pathways and GO terms (c) of upregulated mRNAs. Top 10 significantly enriched KEGG (d) pathways and GO terms (e) of downregulated mRNAs. The x-axis represents the counts of the enriched genes, and the y-axis represents the GO terms or KEGG pathways. The red strip represents high P value. KEGG, Kyoto Encyclopedia of Genes and Genomes; GO, Gene Ontology.

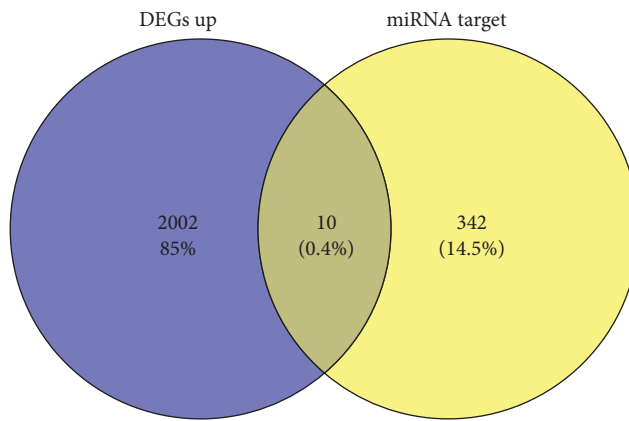
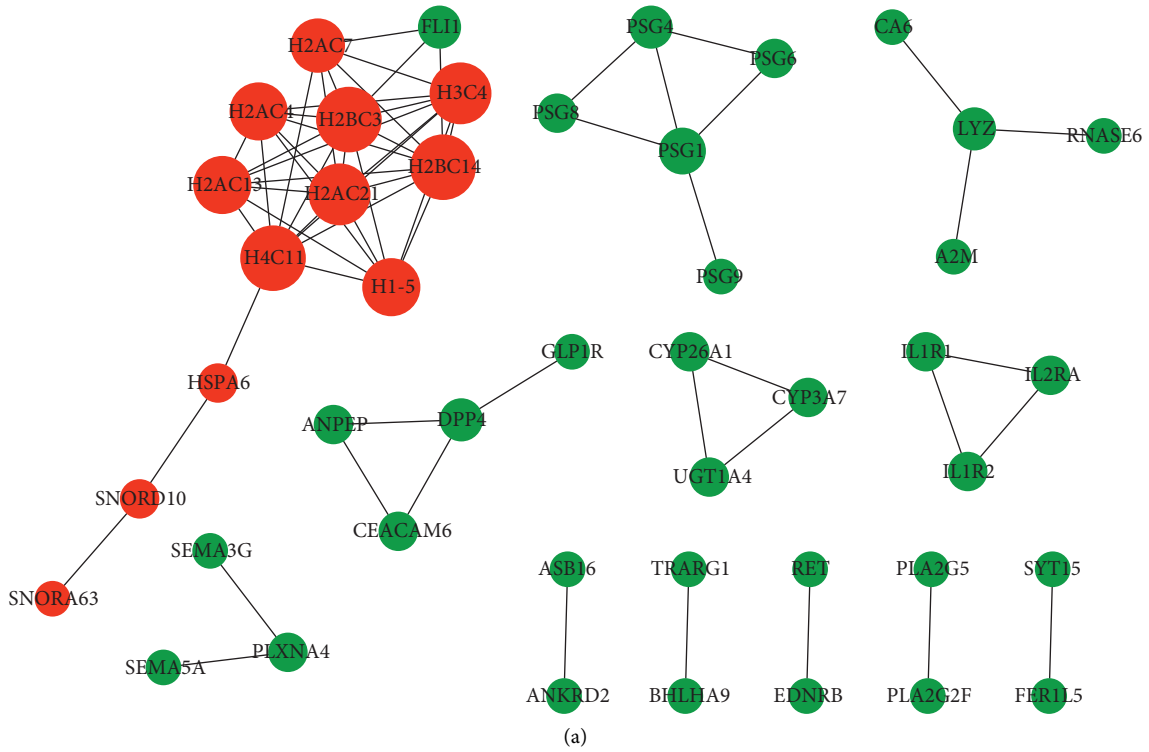


FIGURE 6: Continued.

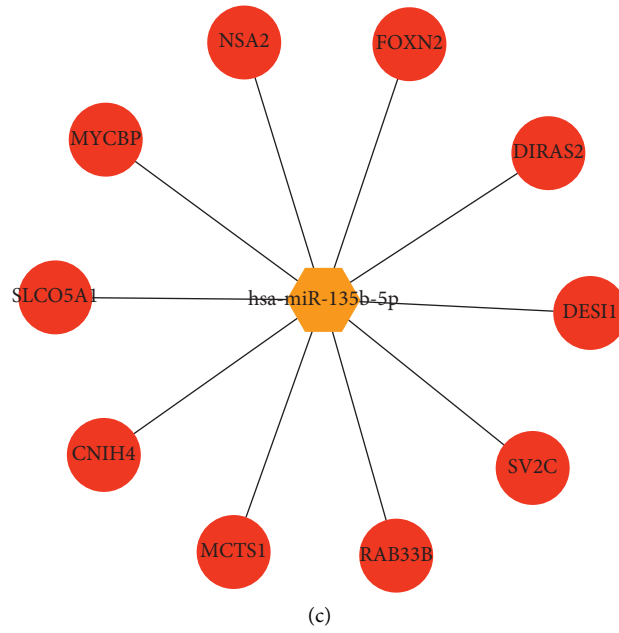


FIGURE 6: PPI network and hsa-miR-135b-5p-target gene regulatory network. (a) PPI network. (b) The overlapped genes. (c) hsa-miR-135b-5p-target gene regulatory network. Red and green colors represent up and downregulated mRNAs, respectively, and a bigger node indicates a higher degree. PPI, protein-protein interaction.

TABLE 2: Degree of nodes in the protein-protein interaction network.

Name	Degree	Betweenness	Closeness	Type
H2BC14	9	8.2	0.030178	Down
H2BC3	9	8.2	0.030178	Down
H4C11	9	55.2	0.03022	Down
H2AC21	8	1.2	0.030158	Down
H3C4	8	1.2	0.030158	Down
H1-5	7	0	0.030137	Down
H2AC4	7	0	0.030137	Down
H2AC13	7	0	0.030137	Down
H2AC7	6	4	0.030116	Down
PSG1	4	7	0.02439	Down
LYZ	3	6	0.02381	Down
DPP4	3	4	0.02381	Down
FLI1	3	0	0.029993	Down
PSG4	3	1	0.024377	Down
ANPEP	2	0	0.023797	Down
CEACAM6	2	0	0.023797	Down
CYP26A1	2	0	0.023256	Up
UGT1A4	2	0	0.023256	Up
CYP3A7	2	0	0.023256	Up
SNORD10	2	22	0.029891	Down
HSPA6	2	40	0.030075	Down
IL1R1	2	0	0.023256	Down
IL1R2	2	0	0.023256	Up
IL2RA	2	0	0.023256	Up
PLXNA4	2	2	0.023256	Up
PSG6	2	0	0.024363	Up
PSG8	2	0	0.024363	Up
A2M	1	0	0.023784	Up
ANKRD2	1	0	0.022727	Up
ASB16	1	0	0.022727	Up

TABLE 2: Continued.

Name	Degree	Betweenness	Closeness	Type
BHLHA9	1	0	0.022727	Up
TRARG1	1	0	0.022727	Down
CA6	1	0	0.023784	Down
GLP1R	1	0	0.023784	Down
EDNRB	1	0	0.022727	Down
RET	1	0	0.022727	Down
SNORA63	1	0	0.02967	Down
FER1L5	1	0	0.022727	Down
SYT15	1	0	0.022727	Down
RNASE6	1	0	0.023784	Down
PLA2G2F	1	0	0.022727	Down
PLA2G5	1	0	0.022727	Down
SEMA3G	1	0	0.023244	Down
SEMA5A	1	0	0.023244	Down
PSG9	1	0	0.02435	Down

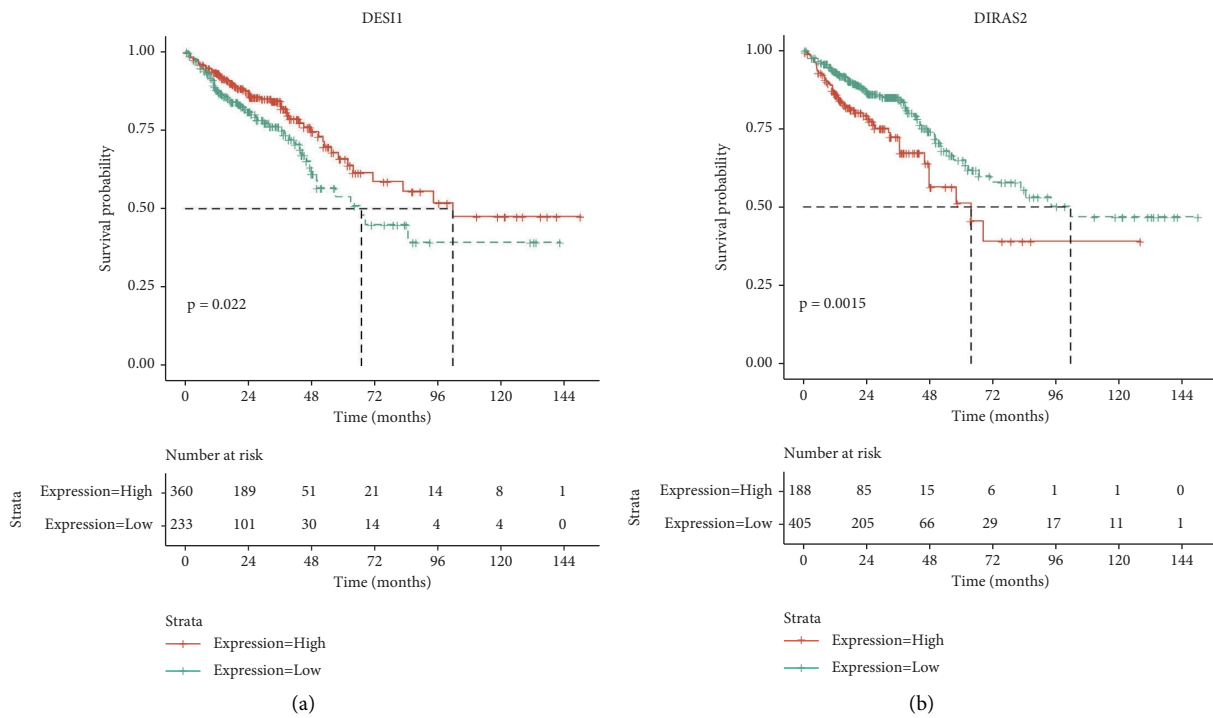


FIGURE 7: Continued.

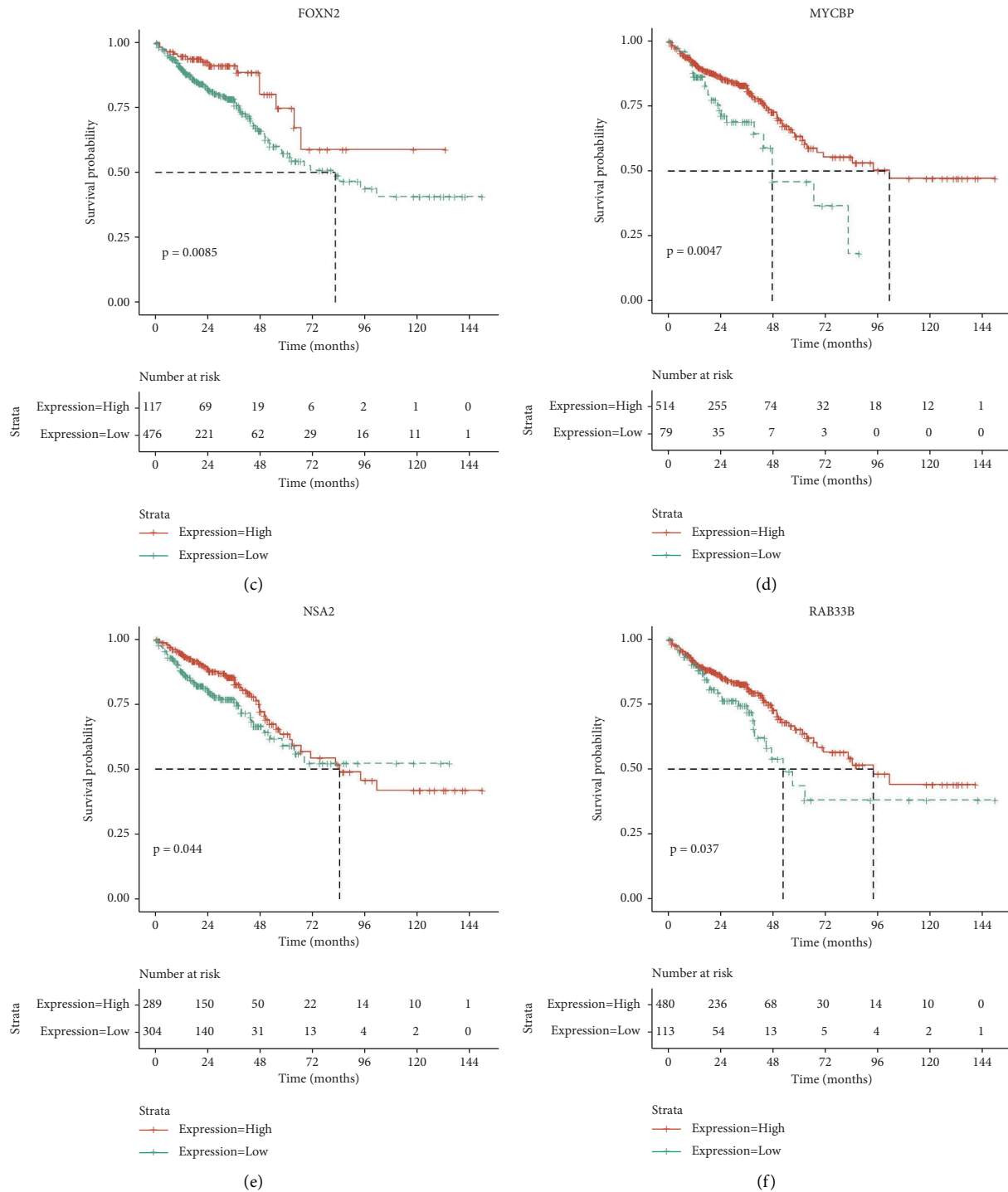


FIGURE 7: Kaplan–Meier survival curves of 10 overlapped genes. (a) *DES11*. (b) *DIRAS2*. (c) *FOXN2*. (d) *MYCBP*. (e) *NSA2*. (f) *RAB33B*.

To understand the exact mechanism underlying the effects of hsa-miR-135b-5p in COAD, transcriptome sequencing was performed. A total of 3384 DEMRNAs were screened, and enrichment analysis showed that the upregulated mRNAs were enriched in 25 KEGG pathways, and the downregulated mRNAs were involved in 20 KEGG pathways, including ribosome, oxidative phosphorylation, and ECM-receptor interaction. Ribosomes are essential for

cellular growth, survival, and proliferation, and disruption of ribosome biogenesis can promote cell cycle arrest; thus, ribosome biogenesis is related to cancer [33]. Many studies have shown that oxidative phosphorylation can be upregulated in cancers and may be used as a target in cancer therapy [34–36]. The ECM is a non-cellular component of tissue, and previous studies have reported that ECM-receptor interactions play an important role in the

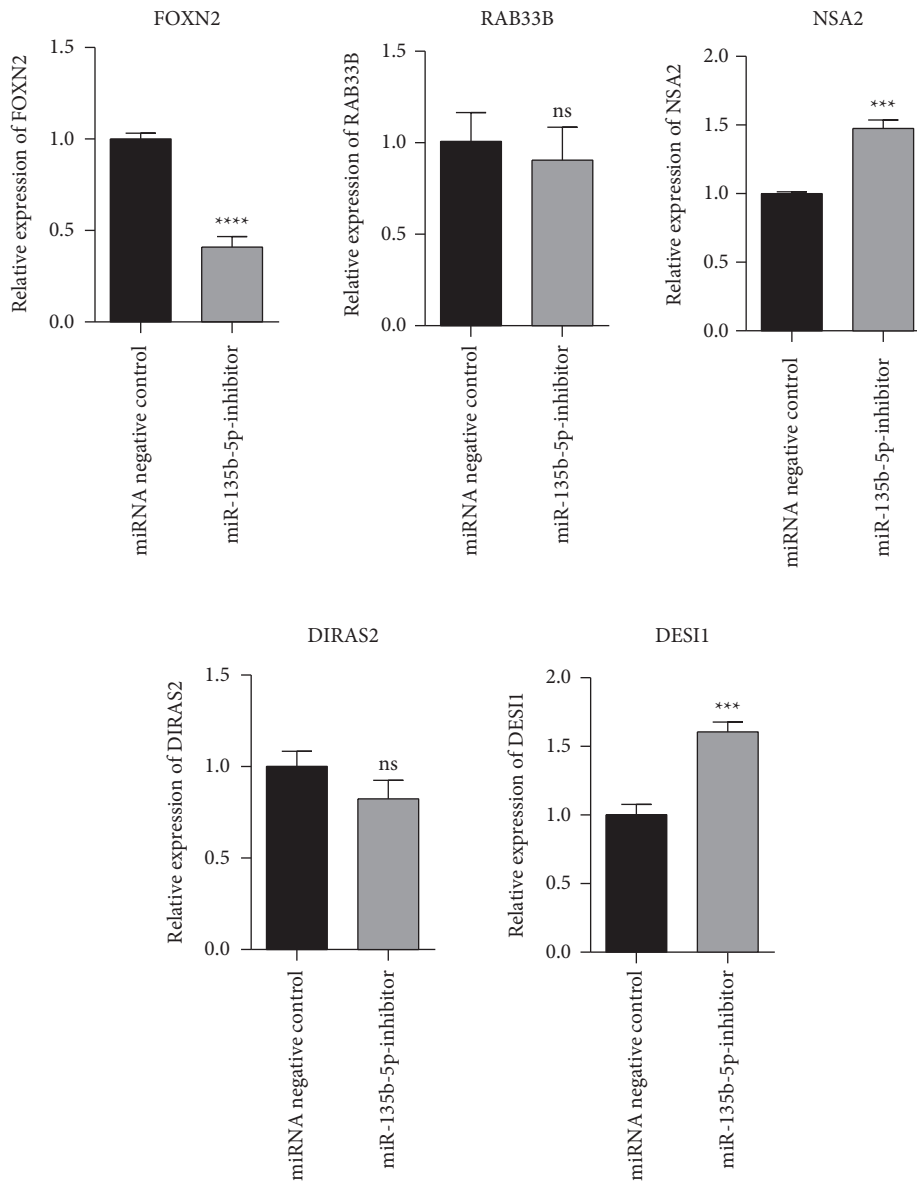


FIGURE 8: Validation analysis of the prognosis-related genes. *** $P < 0.001$, **** $P < 0.0001$, and “ns” represents no significant difference.

development and metastasis of colorectal cancer [37–39]. Thus, we hypothesized that hsa-miR-135b-5p promotes COAD progression via the ribosome, oxidative phosphorylation, and ECM-receptor interaction pathways. Additionally, a PPI network was constructed, and H2BC14 (degree = 9), H2BC3 (degree = 9), and H4C11 (degree = 9) had a higher degree in the network. Valle et al. found that H2BC3, also known as *HIST1H2BB*, has growth-suppressing roles and can be used as a high-grade serous carcinoma precision medicine biomarkers [40]. Meanwhile, only a few studies on H2BC14 and H4C11 in cancer have been reported.

The target genes of hsa-miR-135b-5p were searched and were intersected with the DEmRNAs, resulting in a total of 10 overlapping genes. Prognostic analysis showed that *FOXN2*, *NSA2*, *MYCBP*, *DIRAS2*, *DESI1*, and *RAB33B* had prognostic significance. In addition, the six prognosis-related genes were

validated, and *FOXN2*, *NSA2*, and *DESI1* were found to be significantly expressed between the miR-135b-5p-inhibitor and negative control groups. Ye and Duan found that *FOXN2* is downregulated in breast cancer and modulates invasion, migration, and epithelial-mesenchymal transition via regulation of *SLUG* [41]. Liu et al. reported that *FOXN2* can inhibit the invasion and proliferation of human hepatocellular carcinoma cells [42]. Jeong et al. revealed that HOXC6-mediated miR-188-5p expression induces cell migration by inhibiting the tumor suppressor *FOXN2* [43]. Dai et al. found that the lncRNA WT1-AS inhibits cell aggressiveness via the miR-203a-5p/*FOXN2* axis and is associated with the prognosis of cervical cancer [44]. *NSA2*, also known as *TINP1*, promotes tumor cell proliferation and significantly reduces *p53* and *p21* expression [45]. Wang et al. showed that *NSA2* plays an important role in the development of ovarian cancer [46]. However, further in-depth studies are required to confirm this.

Despite the findings, this study has some limitations. First, additional relevant experiments should be conducted to validate the six prognosis-related genes and pathways identified in this study. Second, further studies are required to analyze the specific mechanisms of hsa-miR-135b-5p in the progression of COAD. Third, the function of hsa-miR-135b-5p should be explored *in vivo*, and the clinical application of miR-135b-5p should be further analyzed.

5. Conclusions

In summary, downregulation of hsa-miR-135b-5p may target *FOXN2*, *NSA2*, and *DESII*, thereby inhibiting cell proliferation, migration, and invasion in COAD. Therefore, hsa-miR-135b-5p can be used as a therapeutic target for COAD treatment.

Data Availability

Data used to support the findings of this study are available from GEO and TCGA database. Transcriptome sequencing data were obtained from the National Center for Biotechnology Information database using the BioProject ID PRJNA870261

Additional Points

Highlights. (1) hsa-miR-135b-5p was highly expressed in COAD. (2) Downregulation of hsa-miR-135b-5p inhibits COAD cell proliferation, migration, and invasion. (3) hsa-miR-135b-5p may promote COAD progression by targeting *FOXN2*, *NSA2*, and *DESII*.

Conflicts of Interest

The authors declare that there are no conflicts of interest regarding the publication of this paper.

References

- [1] R. L. Siegel, K. D. Miller, H. E. Fuchs, and A. Jemal, "Cancer statistics, 2021," *CA: A Cancer Journal for Clinicians*, vol. 71, no. 1, pp. 7–33, 2021.
- [2] J. D. Vogel, S. I. Felder, A. R. Bhama et al., "The American society of colon and rectal surgeons clinical practice guidelines for the management of colon cancer," *Diseases of the Colon & Rectum*, vol. 65, no. 2, pp. 148–177, 2022.
- [3] A. Gurba, P. Taciak, M. Sacharczuk, I. Mlynarczuk-Bialy, M. Bujalska-Zadrozny, and J. Fichna, "Gold (III) derivatives in colon cancer treatment," *International Journal of Molecular Sciences*, vol. 23, no. 2, p. 724, 2022.
- [4] V. Barresi, L. Reggiani Bonetti, A. Ieni, R. A. Caruso, and G. Tuccari, "Histological grading in colorectal cancer: new insights and perspectives," *Histology & Histopathology*, vol. 30, no. 9, pp. 1059–1067, 2015.
- [5] K. Nakamura, R. Seishima, K. Emoto et al., "Development of colon adenocarcinoma on a ganglioneuroma in a patient with nonhereditary disease," *American Journal of Gastroenterology*, vol. 117, no. 7, p. 1028, 2022.
- [6] C. Xia, X. Dong, H. Li et al., "Cancer statistics in China and United States, 2022: profiles, trends, and determinants," *Chinese Medical Journal*, vol. 135, no. 5, pp. 584–590, 2022.
- [7] J. M. Loree and S. Kopetz, "Recent developments in the treatment of metastatic colorectal cancer," *Therapeutic advances in medical oncology*, vol. 9, no. 8, pp. 551–564, 2017.
- [8] A. C. Akinkuotu, U. N. Maduekwe, and A. Hayes-Jordan, "Surgical outcomes and survival rates of colon cancer in children and young adults," *The American Journal of Surgery*, vol. 221, no. 4, pp. 718–724, 2021.
- [9] B. D. Lo, G. Caturegli, M. Stem et al., "The impact of surgical delays on short and long-term survival among colon cancer patients," *The American Surgeon*, vol. 87, no. 11, pp. 1783–1792, 2021.
- [10] T. X. Lu and M. E. Rothenberg, "MicroRNA," *The Journal of Allergy and Clinical Immunology*, vol. 141, no. 4, pp. 1202–1207, 2018.
- [11] Z. Ali Syeda, S. S. S. Langden, C. Munkhzul, M. Lee, and S. J. Song, "Regulatory mechanism of MicroRNA expression in cancer," *International Journal of Molecular Sciences*, vol. 21, no. 5, p. 1723, 2020.
- [12] B. M. Hussien, H. J. Hidayat, A. Salihi, D. K. Sabir, M. Taheri, and S. Ghafouri-Fard, "MicroRNA: a signature for cancer progression," *Biomedicine & Pharmacotherapy*, vol. 138, Article ID 111528, 2021.
- [13] T. Kim and C. M. Croce, "MicroRNA and ER stress in cancer," *Seminars in Cancer Biology*, vol. 75, pp. 3–14, 2021.
- [14] D. M. Hausman, "What is cancer?" *Perspectives in Biology and Medicine*, vol. 62, no. 4, pp. 778–784, 2019.
- [15] M. Xu, Y. Kuang, M. Wang, X. Han, and Q. Yang, "A microRNA expression signature as a predictor of survival for colon adenocarcinoma," *Neoplasma*, vol. 64, no. 01, pp. 56–64, 2017.
- [16] B. Mi, Q. Li, T. Li, G. Liu, and J. Sai, "High miR-31-5p expression promotes colon adenocarcinoma progression by targeting TNS1," *Aging*, vol. 12, no. 8, pp. 7480–7490, 2020.
- [17] Z. Zhao and X. Qin, "MicroRNA-708 targeting ZNF549 regulates colon adenocarcinoma development through PI3K/AKT pathway," *Scientific Reports*, vol. 10, no. 1, Article ID 16729, 2020.
- [18] F. Liu and X. Di Wang, "miR-150-5p represses TP53 tumor suppressor gene to promote proliferation of colon adenocarcinoma," *Scientific Reports*, vol. 9, no. 1, p. 6740, 2019.
- [19] G. K. Smyth, *Limma: Linear Models for Microarray Data. In Bioinformatics and Computational Biology Solutions using R and Bioconductor*, Springer, Berlin, Germany, 2013.
- [20] H. Dweep and N. Gretz, "miRWalk2.0: a comprehensive atlas of microRNA-target interactions," *Nature Methods*, vol. 12, no. 8, p. 697, 2015.
- [21] P. Shannon, A. Markiel, O. Ozier et al., "Cytoscape: a software environment for integrated models of biomolecular interaction networks," *Genome Research*, vol. 13, no. 11, pp. 2498–2504, 2003.
- [22] P. Xia, X. Gao, L. Shao et al., "Down-regulation of RAC2 by small interfering RNA restrains the progression of osteosarcoma by suppressing the Wnt signaling pathway," *International Journal of Biological Macromolecules*, vol. 137, pp. 1221–1231, 2019.
- [23] M. I. Love, W. Huber, and S. Anders, "Moderated estimation of fold change and dispersion for RNA-seq data with DESeq2," *Genome Biology*, vol. 15, no. 12, p. 550, 2014.
- [24] G. Yu, L. G. Wang, Y. Han, and Q. Y. He, "Cluster profiler: an R package for comparing biological themes among gene

- clusters,” *OMICS: A Journal of Integrative Biology*, vol. 16, no. 5, pp. 284–287, 2012.
- [25] D. Szklarczyk, A. Franceschini, S. Wyder et al., “STRING v10: protein-protein interaction networks, integrated over the tree of life,” *Nucleic Acids Research*, vol. 43, no. D1, pp. D447–D452, 2015.
- [26] M. L. Speir, A. S. Zweig, K. R. Rosenbloom et al., “The UCSC Genome Browser database: 2016 update,” *Nucleic Acids Research*, vol. 44, no. D1, pp. D717–D725, 2016.
- [27] T. Therneau and T. Lumley, *Survival: survival analysis, including penalised likelihood*, 2009, <https://CRAN.R-project.org/package=survival>.
- [28] M. Hill and N. Tran, “miRNA interplay: mechanisms and consequences in cancer,” *Disease models & mechanisms*, vol. 14, no. 4, p. dmm047662, 2021.
- [29] Y. S. Lee and A. Dutta, “MicroRNAs in cancer,” *Annual Review of Pathology: Mechanisms of Disease*, vol. 4, no. 1, pp. 199–227, 2009.
- [30] L. D. Naorem, M. Muthaiyan, and A. Venkatesan, “Identification of dysregulated miRNAs in triple negative breast cancer: a meta-analysis approach,” *Journal of Cellular Physiology*, vol. 234, no. 7, pp. 11768–11779, 2019.
- [31] R. Lazzarini, M. Caffarini, G. Delli Carpini, A. Ciavattini, R. Di Primio, and M. Orciani, “From 2646 to 15: differentially regulated microRNAs between progenitors from normal myometrium and leiomyoma,” *American Journal of Obstetrics and Gynecology*, vol. 222, no. 6, 2020.
- [32] L. Magalhães, L. G. Quintana, D. C. F. Lopes et al., “APC gene is modulated by hsa-miR-135b-5p in both diffuse and intestinal gastric cancer subtypes,” *BMC Cancer*, vol. 18, no. 1, p. 1055, 2018.
- [33] Z. Turi, M. Lacey, M. Mistrik, and P. Moudry, “Impaired ribosome biogenesis: mechanisms and relevance to cancer and aging,” *Aging*, vol. 11, no. 8, pp. 2512–2540, 2019.
- [34] T. M. Ashton, W. G. McKenna, L. A. Kunz-Schughart, and G. S. Higgins, “Oxidative phosphorylation as an emerging target in cancer therapy,” *Clinical Cancer Research*, vol. 24, no. 11, pp. 2482–2490, 2018.
- [35] V. Sica, J. M. Bravo-San Pedro, G. Stoll, and G. Kroemer, “Oxidative phosphorylation as a potential therapeutic target for cancer therapy,” *International Journal of Cancer*, vol. 146, no. 1, pp. 10–17, 2020.
- [36] C. Ge, Y. Wang, Y. Feng et al., “Suppression of oxidative phosphorylation and IDH2 sensitizes colorectal cancer to a naphthalimide derivative and mitoxantrone,” *Cancer Letters*, vol. 519, pp. 30–45, 2021.
- [37] S. Crotti, M. Piccoli, F. Rizzolio, A. Giordano, D. Nitti, and M. Agostini, “Extracellular matrix and colorectal cancer: how surrounding microenvironment affects cancer cell behavior?” *Journal of Cellular Physiology*, vol. 232, no. 5, pp. 967–975, 2017.
- [38] V. Stankevicius, G. Vasauskas, R. Noreikiene, K. Kuodyte, M. Valius, and K. Suziedelis, “Extracellular matrix-dependent pathways in colorectal cancer cell lines reveal potential targets for anticancer therapies,” *Anticancer Research*, vol. 36, no. 9, pp. 4559–4568, 2016.
- [39] D. V. Maltseva and S. A. Rodin, “Laminins in metastatic cancer,” *Molecular Biology*, vol. 52, no. 3, pp. 350–371, 2018.
- [40] B. L. Valle, S. Rodriguez-Torres, E. Kuhn et al., “HIST1H2BB and MAGI2 methylation and somatic mutations as precision medicine biomarkers for diagnosis and prognosis of high-grade serous ovarian cancer,” *Cancer Prevention Research*, vol. 13, no. 9, pp. 783–794, 2020.
- [41] H. Ye and M. Duan, “FOXN2 is downregulated in breast cancer and regulates migration, invasion, and epithelial–mesenchymal transition through regulation of SLUG,” *Cancer Management and Research*, vol. 11, pp. 525–535, 2019.
- [42] X. H. Liu, L. P. Liu, X. M. Xu et al., “FOXN2 suppresses the proliferation and invasion of human hepatocellular carcinoma cells,” *European Review for Medical and Pharmacological Sciences*, vol. 25, no. 2, pp. 731–737, 2021.
- [43] S. Jeong, S. A. Kim, and S. G. Ahn, “HOXC6-Mediated miR-188-5p expression induces cell migration through the inhibition of the tumor suppressor FOXN2,” *International Journal of Molecular Sciences*, vol. 23, no. 1, p. 9, 2021.
- [44] S. G. Dai, L. L. Guo, X. Xia, and Y. Pan, “Long non-coding RNA WT1-AS inhibits cell aggressiveness via miR-203a-5p/FOXN2 axis and is associated with prognosis in cervical cancer,” *European Review for Medical and Pharmacological Sciences*, vol. 23, no. 2, pp. 486–495, 2019.
- [45] W. Li, A. P. Song, F. Zhao, Y. M. Hu, and M. Hua, “A novel human TINP1 gene promotes cell proliferation through inhibition of p53 and p21 expression,” *Oncology Reports*, vol. 30, no. 4, pp. 1848–1852, 2013.
- [46] X. Wang, Y. Wang, F. Sun et al., “Novel LncRNA ZFH4-AS1 as a potential prognostic biomarker that affects the immune microenvironment in ovarian cancer,” *Frontiers in Oncology*, vol. 12, Article ID 945518, 2022.